BACHELOR

The damping of Faraday waves due to a monomolecular oil film

Merks, J.

Award date:
2010

The damping of Faraday waves due to a monomolecular oil film

Johan Merks

December 2010
R-1800-S

Technische Universiteit
Eindhoven
University of Technology

Department of Applied Physics

Den Dolech 2, 5612 AZ Eindhoven
P.O. Box 513, 5600 MB Eindhoven
The Netherlands
www.tue.nl

Author
Johan Merks

Reference
R-1800-S

Date
December 21, 2011

The damping of Faraday waves due to a monomolecular oil film

Abstract

The damping of surface waves due to an oil film is known since ancient times. Many attempts have been made to explain this phenomenon, but it is still unknown what really physically happens in the system of a monomolecular film on water. This work provides a theoretical and experimental study of the damping of surface waves for both water with a pure surface and water covered with a monomolecular layer of silicon oil. For the experimental section a vertically oscillated fluid container is used to create Faraday waves. Using shadowgraphy the temporal damping is measured. It was found that the critical amplitude for water with a pure surface is higher compared to that of the mono-layer case. The temporal damping coefficient of water covered with a monomolecular oil film was found to be smaller than the temporal damping coefficient of water with a pure surface, however the opposite was expected according to the theory.

Technische Universiteit
Eindhoven
University of Technology

Table of contents

Title
The damping of Faraday waves due to a monomolecular oil film

1 Introduction

> *I had, when a youth, read and smiled at Pliny's account of a practice among the seaman of his time, to still the waves in a storm by pouring oil into the sea....* [5]

The words above are extracted from a letter to Dr William Brownrigg written by Benjamin Franklin. Franklin refers to the writing of Caius Plinius Secundus (Pliny the Elder) in his *Historia Naturalis*. In the letter the first recorded scientific experiment of the damping of waves due to oil films is described [6].

> *In 1757, being at sea in a fleet of 96 sail bound against Louisburg, I observed the wakes of two of the ships to be remarkably smooth, while the others were ruffled by the wind, which blew fresh. Being puzzled with the differing appearance, I at last pointed it out to our captain, and asked him the meaning of it? "The cooks", says he, "have, I suppose, been just emptying their greasy water through the scuppers, which has greased the sides of those ships a little"; and this answer he gave me with an air of some little contempt as to a person ignorant of what everybody else knew. In my own mind I at first slighted his solution, tho' I was not able to think of another. But recollecting what I had formerly read in Pliny, I resolved to make some experiment of the effect of oil on water, when I should have opportunity.....*
>
> *At length being at Clapham where there is, on the common, a large pond, which I observed to be one day very rough with the wind, I fetched out a cruet of oil, and dropt a little of it on the water. I saw it spread itself with surprising swiftness upon the surface; but the effect of smoothing the waves was not produced; for I had applied it first on the leeward side of the pond, where the waves were largest, and the wind drove my oil back upon the shore. I then went to the windward side, where they began to form; and there the oil, though not more than a teaspoonful, produced an instant calm over a space several yards square, which spread amazingly, and extended itself gradually till it reached the lee side, making all that quarter of the pond, perhaps half an acre, as smooth as a looking-glass* [5].

In an attempt to explain the damping effect Franklin writes:

> *Now I imagine that the wind blowing over water thus covered with a film of oil, cannot easily catch upon it, so as to raise the first wrinkles, but slides over it, and leaves it smooth as it finds it. It moves a little the oil indeed, which, being between it and the water, serves it to slide with, and prevents friction, as oil does between those parts of a machine that would otherwise rub hard together* [5].

The effect of the damping of water waves due to oil films has been known since ancient times. Intrigued by among other things Franklin's account many attempts to explain this phenomenon were made, but it is still unknown what really physically happens in the system of a monomolecular film on water. Figure 1.1 shows an example of the Franklin experiment described above [15].

In this report a theory of the wave damping is provided. The damping of water with a monomolecular film of silicon oil is measured and compared with the damping of water. In the experiment Faraday waves, standing waves that are induced on the surface of a liquid that is subjected to the oscillating vertical displacement of the liquid-container, are used. Shadowgraphy is used to obtain intensity images of the wave patterns. The intensity of the images is calculated, which is a measure of the amplitude of the waves.

Figure 1.1: Recreated Franklin experiment. The upper photo shows the water condition prior to the addition of oil. The lower picture shows the condition after the addition of oil [15]
.

2 Theory

In this chapter the wave motion and damping at a pure liquid-vapor interface are described. Furthermore a theory for the damping of capillary waves on a liquid surface covered by a insoluble monolayer is presented [13, 11, 9]. In the experiment the temporal damping of the capillary waves is measured. However most literature describe the spatial damping, as waves damped as function of distance are more easily accessible to measurements than waves damped as function of time [13]. Therefore both damping mechanisms are discussed.

2.1 Damping of capillary waves on a pure liquid-vapor interface

2.1.1 Wave motion

First the propagation of capillary waves at a liquid-vapor interface is described. Consider a container which contains a fluid layer of depth h. The bottom of the fluid is located at $z = -h$. The fluid is assumed incompressible and Newtonian. At rest the surface of the fluid is at $z = 0$. Now, the container is subjected to the periodic oscillation $z = a\cos(\Omega t)$ (Figure 2.1). Here a is the amplitude and Ω the angular frequency of the excitation. The equation of the motion of the fluid layer can be described with the Navier-Stokes equation [3, 16, 11]:

$$\frac{\partial \mathbf{u}}{\partial t} + (\mathbf{u}\cdot\nabla)\mathbf{u} = -\frac{1}{\rho}\nabla p + \nu\nabla^2\mathbf{u} + \mathbf{g}, \tag{2.1}$$

and the equation of continuity,

$$\nabla\cdot\mathbf{u} = 0. \tag{2.2}$$

Here, $\mathbf{u} = (u, v, w)$ is the velocity field, $p(x, y, z, t)$ the pressure, ρ the density, $\nu = \eta/\rho$ the kinematic viscosity, with η the shear viscosity of the bulk liquid, and $\mathbf{g} = (-g - a\cos(\Omega t))\hat{e}_z$ the effective gravity.

First an ideal fluid is considered to simplify the equations above. In this case there is no energy dissipation due to viscosity, so the $\nu\nabla^2\mathbf{u}$ term can be omitted from equation 2.1. Fur-

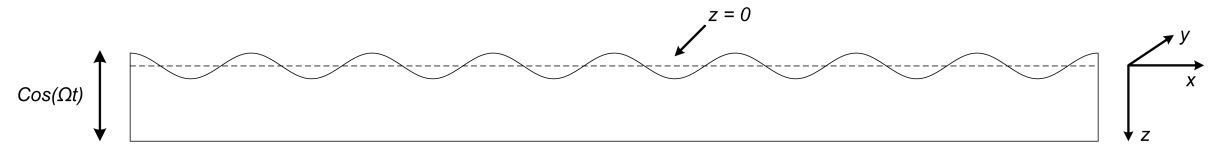

Figure 2.1: Faraday waves

thermore, in the limit where the amplitude of the wave is small compared with the wavelength, the $(\mathbf{u}\cdot\nabla)\mathbf{u}$ term can be neglected, and equation 2.1 can be written as

$$\rho\frac{\partial \mathbf{u}_0}{\partial t} = \nabla p_0 + \rho\mathbf{g}, \tag{2.3}$$

where $\mathbf{u}_0$ is the velocity vector of the wave for an ideal liquid and p_0 the hydrostatic pressure at the interface [9]. Equation 2.3 can be solved using a velocity potential ϕ, defined by

$$\mathbf{u}_0 = \nabla\phi. \tag{2.4}$$

According to the boundary conditions the velocity is zero at the bottom of the liquid:

$$w_0 = \frac{\partial\phi}{\partial z} = 0, \quad z = -h. \tag{2.5}$$

At the surface we require that the liquid moves with the surface,

$$\frac{D\zeta}{Dt} = \frac{\partial\zeta}{\partial t} + u_0\frac{\partial\zeta}{\partial x} = w_0(z=\zeta) = \left.\frac{\partial\phi}{\partial z}\right|_{z=\zeta}, \tag{2.6}$$

where ζ is the vertical displacement of the fluid. For small wave amplitudes only the linear terms are retained,

$$\frac{\partial\zeta}{\partial t} = \left.\frac{\partial\phi}{\partial z}\right|_{z=\zeta} \approx \left.\frac{\partial\phi}{\partial z}\right|_{z=0}. \tag{2.7}$$

For a rotation free flow $\partial\mathbf{u}_0/\partial t = \nabla\partial\phi/\partial t$. If we put this into the Bernoulli equation $\frac{1}{2}u_0^2 + p_0/\rho + gz =$ constant, we obtain

$$\frac{\partial\phi}{\partial t} + \frac{1}{2}u_0^2 + \frac{p_0}{\rho} + gz = \text{constant}. \tag{2.8}$$

With $p = 0$ at $z = \zeta$ the linear terms of this equation give

$$\frac{\partial\phi}{\partial t} + g\zeta = 0. \tag{2.9}$$

Now we have:

$$\frac{\partial^2\phi}{\partial x^2} + \frac{\partial^2\phi}{\partial z^2} = 0 \tag{2.10}$$

$$\frac{\partial\phi}{\partial z} = 0, \quad z = -h \tag{2.11}$$

$$\frac{\partial\zeta}{\partial t} = \frac{\partial\phi}{\partial z}, \quad z = 0 \tag{2.12}$$

$$\frac{\partial\phi}{\partial t} = -g\zeta, \quad z = 0. \tag{2.13}$$

Now we try a harmonic solution, $\zeta(x,t) = ae^{i(k_0x-\omega_0t)}$ and $\phi(x,z,t) = f(z)e^{i(k_0x-\omega_0t)}$, with $k_0 = 2\pi/\lambda$ the wavevector, λ the wavelength and ω_0 the angular frequency. The quantities k_0, λ and ω_0 are real. Equation 2.12 gives

$$\frac{d^2f}{dz^2} - k_0^2 f = 0, \tag{2.14}$$

$$f(z) = (Ae^{k_0z} + Be^{-k_0z}), \tag{2.15}$$

from which we keep the finite solution for a infinite deep fluid, so $B = 0$. If this solution is used in equation 2.13, we obtain

$$kA = a\omega_0, \tag{2.16}$$

$$\phi = a\frac{\omega_0}{k_0}e^{k_0 z}e^{i(k_0 x - \omega_0 t)}. \tag{2.17}$$

Using this in equation 2.13 results in $\omega_0^2/k_0 = g$.

Now the surface tension is taken into account, using the following boundary condition:

$$p_0 - p_v = \frac{\sigma}{r} = p_\sigma, \tag{2.18}$$

where p_v is the pressure of the vapor. The curvature r of the surface is

$$\frac{1}{r} = \frac{-\partial^2\zeta/\partial x^2}{(1 + (\partial\zeta/\partial x)^2)^2} \approx \frac{\partial^2\zeta}{\partial x^2}, \tag{2.19}$$

and p_σ is now given by the Laplace-Young equation

$$p_\sigma = \sigma\frac{\partial^2\zeta}{\partial x^2}. \tag{2.20}$$

Using this in equation 2.9 gives

$$\frac{\partial\phi}{\partial t} - \frac{\sigma}{\rho}\frac{\partial^2\zeta}{\partial x^2} + g\zeta = 0. \tag{2.21}$$

Which follows is the dispersion relation

$$\omega_0^2 = gk_0 + \frac{\sigma}{\rho}k_0^3, \tag{2.22}$$

which is known as the Kelvin equation [9].

2.1.2 Including viscosity

The wave motion of an ideal fluid was discussed in the previous section. In reality, however, waves are weakened due to viscosity. Therefore, the dispersion relation of viscous fluids is more complicated than the Kelvin equation (equation 2.22). With the use of the equation of continuity, equation 2.2, and the linearized Navier-Stokes equation,

$$\frac{\partial\mathbf{u}}{\partial t} = \frac{1}{\rho}\nabla p + \nu\nabla^2\mathbf{u} + g, \tag{2.23}$$

the wave motion for a viscous liquid can be described. The solutions for the wave motion are simplified by considering that the liquid velocity is given by a vector field in space and that any such a field can be expressed as the sum of a rotation free and a divergence free field [13]:

$$u = u_0 + u_1, \tag{2.24}$$

$$w = w_0 + w_1, \tag{2.25}$$

$$p = p_0, \tag{2.26}$$

where

$$\nabla \times u_0 = \nabla \times w_0 = 0 \tag{2.27}$$

$$\nabla \cdot u_1 = \nabla \cdot w_1 = 0 \tag{2.28}$$

Here, p_0, u_0 and w_0 are the results obtained from an ideal liquid. The changes introduced by the presence of viscosity are represented by u_1 and w_1.

The rotation free field can be characterized with a potential ϕ as $\mathbf{u}_0 = -\nabla\phi$ and the divergence free field can be described by a vorticity function ψ as $\mathbf{u}_1 = \nabla \times \psi$. Thus the velocity components can be written as:

$$u = -\frac{\partial\phi}{\partial x} - \frac{\partial\psi}{\partial z}, \tag{2.29}$$

$$w = -\frac{\partial\phi}{\partial z} + \frac{\partial\psi}{\partial x}. \tag{2.30}$$

The solutions for ϕ and ψ are in the form [13]

$$\phi = Ae^{kz}e^{i(kx-\omega t)}, \tag{2.31}$$

$$\psi = Ce^{lz}e^{i(kx-\omega t)}, \tag{2.32}$$

where k and ω are complex quantities and l is the rate which the waves diminish with increasing distance into the bulk from the interface.

The velocity components at the interface, $z = 0$, are found by substituting equations 2.31 and 2.32 into equations 2.29 and 2.30:

$$u = (ikAe^{kz} - lCe^{lz})e^{i(kx-\omega t)}, \tag{2.33}$$

$$w = (kAe^{kz} + kCe^{lz})e^{i(kx-\omega t)}, . \tag{2.34}$$

To complete this analysis the following boundary conditions are needed [8]:

$$p_{zx} = 0, \tag{2.35}$$

$$p_{zz} + p_\sigma = p_v, \tag{2.36}$$

where p_{zx} is the tangential and p_{zz} is the normal component of the viscous stress tensor at the surface of the viscous liquid. In the case of a vapor phase the pressure p_v is negligible compared to the capillary pressure p_σ, which is equal to equation 2.20 [9]. By substituting equations 2.33 and 2.34 into the boundary conditions 2.35 and 2.36 a relation between A and C can be provided:

$$(\omega^2 - i2\nu k^2\omega + gk + \frac{\sigma}{\rho}k^3)A + i(gk + \frac{\sigma}{\rho}k^3 - i2\nu lk\omega)C = 0, \tag{2.37}$$

$$i2\nu k^2 A - (2\nu k^2 - i\omega)C = 0. \tag{2.38}$$

By equating the determinant of equations 2.37 and 2.38 to zero, a relation for the angular frequency ω and wavevector k for a free surface of a viscous fluid is found:

$$(2\nu k^2 + i\omega)^2 + \omega^2 = 4\nu^2 k^4 (1 - \frac{i\omega}{\nu k^2})^{\frac{1}{2}}, \tag{2.39}$$

which is the Lamb-Levich dispersion relation [11],[9].

2.1.3 Surface wave damping

The damping of surface waves is the result of energy dissipation due to viscosity. In equations 2.33 and 2.34 A is the amplitude of the velocity potential for the ideal fluid and C is the amplitude as a result of the viscous contribution. The ratio A/C is a measure of how viscous the fluid is. For the low-viscosity limit, the deviation of the wave motion from the ideal case is small and therefore the ratio A/C is large. From equation 2.38 this ratio can be obtained:

$$\frac{A}{C} = -i(1 - i\frac{\omega}{2\nu k^2}). \tag{2.40}$$

For this ratio to be large

$$\frac{\omega}{2\nu k^2} \gg 1 \tag{2.41}$$

must be satisfied. For high viscous liquids the above inequality is reversed [9].

As mentioned in the beginning of the chapter two different damping mechanisms will be discussed, wave damping as function of the distance from the wave-generating source, the spatial damping, and the decay of waves as function of time, the temporal damping. To study the spatial damping, surface waves with a real angular frequency ω_0 are used. The complex wavevector k can be described as

$$k = k_0 + i\alpha, \tag{2.42}$$

where α is the spatial damping coefficient and $\alpha \gg k_0$. By substituting the angular frequency ω_0 and equation 2.42 into equation 2.39, α can be obtained. For short wavelengths the gravitational contribution in the Lamb-Levich dispersion relation can be neglected [11]. By retaining only the first order terms in α and ν the following relation is obtained:

$$\frac{4\eta}{\rho}k_0^2\omega_0 - \frac{3\sigma}{\rho}\alpha k_0^2 = 0. \tag{2.43}$$

From this immediately follows that the spatial damping coefficient for capillary waves of angular frequency ω_0, propagating in a free surface of a low-viscosity fluid is given by

$$\alpha = \frac{4\eta\omega_0}{3\sigma}. \tag{2.44}$$

By substituting equation 2.44 into 2.42 the wavevector is obtained [9]:

$$k = (\frac{\rho\omega_0^2}{\sigma})^{\frac{1}{3}} - i\frac{4\eta\omega_0}{3\sigma}. \tag{2.45}$$

For obtaining the temporal damping of capillary waves the wavevector $k = k_0$ is real and the angular frequency ω is complex. The angular frequency can be written as

$$\omega = \omega_0 - i\beta, \tag{2.46}$$

with β the temporal damping coefficient and $\beta \gg \omega_0$. By substituting equation 2.46 and k_0 into the Lamb-Levich dispersion relation, neglecting the gravity contribution for short wavelength waves as before and retaining only the first order terms of β and ν, the following is found:

$$i2\beta\omega_0 - i4\nu k_0^2\omega_0 = 0. \tag{2.47}$$

From here the temporal damping coefficient for capillary waves with wavevector k_0 at a free surface of a low-viscosity liquid is obtained:

$$\beta = 2\nu k_0^2. \tag{2.48}$$

The angular frequency is found by substituting equation 2.48 into 2.46:

$$\omega = (\frac{\sigma k_0^3}{\rho})^{\frac{1}{2}} - i2\nu k_0^2. \tag{2.49}$$

From equations 2.45 and 2.49 it follows that the spatial and temporal damping coefficients for capillary waves in the low-viscosity regime are related by

$$\alpha = \frac{\beta}{u_g}, \tag{2.50}$$

with

$$u_g = \frac{\partial \omega_0}{\partial k_0} = \frac{3}{2}(\frac{\sigma}{\rho}k_0)^{\frac{1}{2}} \tag{2.51}$$

the group velocity of the surface waves [13, 9].

2.2 Damping of capillary waves at liquid surfaces covered with a insoluble monolayer

Adding a monolayer to a liquid surface has a drastic effect on te damping. This is caused because of the viscous and elastic properties of the monolayer, which resists the periodic expansion and compression of the surface. In this section a theory is provided for the damping of capillary waves on a liquid surface covered by a insoluble monolayer.

2.2.1 Historical account

As written in the introduction, the first recorded experiment of the damping of waves due to an oil layer was carried out by Benjamin Franklin. His explanation was that the oil smooths out the water waves, like oil prevents friction in a machine [5]. Since then, many attempts were made to explain this phenomenon. In 1883 Aiken showed that the increase of surface wave damping by a surface film is due to the film's resistance to compression [1]. In 1890 Rayleigh realized that the thickness of the oil layer of Franklin's experiment was in the order of molecular dimensions [17]. Levich showed that the presence of a monomolecular film at a liquid-vapor interface changes the viscoelastic properties of the surface, which alters the boundary condition of the problem and leads to an increased damping of surface waves [10]. Theoretical studies have also shown that the calming of surface waves in the presence of a monolayer with finite dilational compressibility is due to the suppressed capillary wave generation, which results in a reduced coupling between the liquid surface and the wind [9].

In section 2.1.2 we showed that the tangential and normal components of the viscous stress tensor, equations 2.35 and 2.36, are required to be continuous. The normal component, p_{zz},

is equal to the capillary pressure given by the Laplace-Young equation 2.20, and is the same for both a pure interface as one with a surfactant monolayer. The tangential component only exists when there is a surface tension gradient at the interface. Since there can be no gradients in the surface tension for a pure interface, the tangential component then vanishes. At monolayer covered surfaces the wave motion causes the monolayer to contract and expand, which results in surface tension variations and thus a tangential component of the surface stress tensor exists [10, 9].

The surface viscoelastic properties caused due to the presence of a monolayer can be expressed by two moduli, the surface dilational modulus and the surface shear modulus [13]. The surface dilational modulus is a measure of the surface film's resistance to changes in surface area, represented by the surface dilational elasticity ϵ_d and surface dilational viscosity η_d. The surface shear modulus is a measure of the resistance to changes in the shape of the surface, represented by the surface shear elasticity ϵ_s and surface shear viscosity η_s. In general, the effects of the surface shear modulus are assumed to be small compared to those of the dilational modulus. If the effects of the surface shear modulus are neglected, the only new viscoelastic coefficients are ϵ_d and η_d. For a number of insoluble monolayers has been observed that the surface dilational viscosity is negligible [13]. Then the surface dilational modulus is given by the surface dilational elasticity alone,

$$\epsilon = \epsilon_d(\omega). \tag{2.52}$$

In the static limit, where the surface dilational elasticity is frequency independent, the surface dilational elasticity is equal to the static elasticity, $\epsilon_d = \epsilon_0$. This static elasticity follows from the equilibrium relationship between the surface tension σ and the surface concentration of surfactant molecules Γ_0 [4]:

$$\epsilon_0 = -\frac{\partial \sigma}{\partial \ln \Gamma_0}. \tag{2.53}$$

The surface dilational modulus is therefore directly related to measurable equilibrium surface properties in the purely elastic case.

These new viscoelastic properties alter the boundary conditions of the wave motion. In the next section these boundary conditions are used to describe the wave motion for waves on a surface covered with an insoluble monolayer.

2.2.2 Wave motion of waves covered with an insoluble monolayer

In this section the velocity components of the surface wave and a dispersion relation for waves covered with a monomolecular film are obtained. The solutions for the case of a pure surface obtained in section 2.1 will be used for the monolayer covered surface, however the boundary conditions are different. The normal component of the boundary condition is still given by the Laplace-Young equation, equation 2.20. Neglecting the pressure due to the vapor phase above the liquid as before gives

$$p_{zz} = \sigma(\Gamma)\frac{\partial^2 \zeta}{\partial x^2}. \tag{2.54}$$

The surface tension $\sigma(\Gamma)$ is now a function of the surface concentration Γ and the vertical displacement of the surface from the equilibrium position ζ is defined as

$$\frac{\partial \zeta}{\partial t} = w. \tag{2.55}$$

By using w from equation 2.34, ζ can be written as

$$\zeta = \frac{kA + ikC}{-i\omega} e^{i(kx-\omega t)}. \tag{2.56}$$

Because of the additional viscoelastic properties introduced by the monolayer, the boundary condition given by the tangential component of the viscous stress tensor is no longer zero [9]:

$$p_{zx} = \frac{\partial \sigma}{\partial \Gamma} \frac{\partial \Gamma}{\partial x}, \tag{2.57}$$

where Γ is dependent of the position on the surface and can be written as

$$\Gamma = \Gamma_0 + \Gamma', \tag{2.58}$$

where Γ_0 is the equilibrium surface concentration and $\Gamma' \ll \Gamma_0$ the deviation from the equilibrium value. The surface concentration has to satisfy conservation of mass [11]:

$$\frac{\partial \Gamma}{\partial t} + \frac{\partial}{\partial x}(\Gamma u) = D_s \frac{\partial^2 \Gamma}{\partial x^2}, \tag{2.59}$$

with D_s the surface diffusion coefficient. The solution for the surface concentration deviation is in the form

$$\Gamma' = E e^{i(kx-\omega t)}. \tag{2.60}$$

By substituting equation 2.33 into 2.58 and neglecting all terms of second order contribution, an expression is obtained for the E in equation 2.60:

$$E = \frac{-ik\Gamma_0(ikA - lC)}{-i\omega + k^2 D_s}. \tag{2.61}$$

The $k^2 D_s$ term is small compared to the wave frequency for frequencies in the capillary wave regime, so the surface concentration can be written as

$$\Gamma = \Gamma_0 + \frac{ik\Gamma_0(ikA - lC)}{i\omega} e^{i(kx-\omega t)}. \tag{2.62}$$

By substituting equations 2.62 and 2.56 into 2.54 and approximating $\sigma(\Gamma) \approx \sigma(\Gamma_0)$, the normal boundary condition becomes

$$p_{zz} = \sigma(\Gamma_0) \frac{kA + ikC}{-i\omega} e^{i(kx-\omega t)}. \tag{2.63}$$

The tangential boundary condition can now be written as

$$p_{zx} = \frac{\epsilon k^2}{i\omega}(ikA - lC) e^{i(kx-\omega t)}, \tag{2.64}$$

where the surface dilational modulus ϵ is defined as

$$\epsilon \equiv -\frac{\partial \sigma}{\partial \Gamma}\Gamma_0. \tag{2.65}$$

By equating equations 2.63 and 2.64 to the definitions of the normal and the tangential boundary conditions given by

$$p_{zz} \equiv -p + 2\eta\frac{\partial w}{\partial z}, \tag{2.66}$$

$$p_{zx} \equiv \eta(\frac{\partial u}{\partial w} + \frac{\partial w}{\partial u}), \tag{2.67}$$

and substituting them into equations 2.33 and 2.34, the following two equations relating the unknown quantities A and C are obtained [9]:

$$(-\omega^2 - i\omega 2\nu k^2 + gk + \frac{\sigma}{\rho}k^3)A + i(gk + \frac{\sigma}{\rho}k^3 - i\omega 2\nu kl)C = 0, \tag{2.68}$$

$$i(-i\omega 2\nu k^2 + \frac{\epsilon}{\rho}k^3)A - (-i\omega 2\nu k^2 - \omega^2 + \frac{\epsilon}{\rho}k^2 l)C = 0. \tag{2.69}$$

The gravity terms are negligible in the capillary wave regime. Neglecting these terms and equating the determinant of the equations above to zero, the following dispersion relation for a monolayer covered surface is obtained:

$$(\frac{\sigma}{\rho}k^3 - i\omega 2\nu kl)(-i\omega 2\nu k^2 + \frac{\epsilon}{\rho}k^3) - (-i\omega 2\nu k^2 - \omega^2 + \frac{\epsilon}{\rho}k^2 l)(-\omega^2 - i\omega 2\nu k^2 + \frac{\sigma}{\rho}k^3) = 0 \tag{2.70}$$

The Lamb-Levich dispersion relation, equation 2.39, is recovered by setting the surface dilational modulus ϵ to zero. In the general case the dispersion relation for a surface covered with an insoluble monolayer is a sixth-order polynomial in k [9]:

$$\frac{\epsilon\sigma}{\rho^2}k^6 + \omega^4 + i4\nu k^2\omega - \frac{\epsilon}{\rho}k^2 l\omega^2 - \frac{\sigma}{\rho}k^3\omega^2 + \frac{\epsilon\sigma}{\rho^2}k^5 l = 0. \tag{2.71}$$

2.2.3 Surface wave damping of waves covered with an insoluble monolayer

The imaginary parts of the complex quantities ω and k in the dispersion relation 2.71 represent the damping of the wave motion. As for the pure surface case, only low viscosity liquids will be concerned, so

$$\frac{\omega}{2\nu k^2} \gg 1. \tag{2.72}$$

First the spatial damping will be considered, and as for the pure case the waves have a angular frequency ω_0 and complex wavevector k. In the low-viscosity limit, k differs only slightly from the real value k_0 of the pure case, given by equation 2.22, and can be written as

$$k = k_0 + k', \tag{2.73}$$

where $k' = k'' + i\alpha$ represents the change in wavevector from the pure case. The real part of k' represents changes in the wavelength of the surface in the presence of a monolayer and $\alpha \ll k_0$ is the spatial damping coefficient [9].

By substituting equation 2.73 into the dispersion relation 2.71 and setting $\omega = \omega_0$, the spatial damping coefficient α can be obtained. In the low-viscosity limit given by equation 2.72 the factor l, which was introduced in equation 2.32 and which appears in the dispersion relation 2.71, reduces to

$$l \approx k_0 (\frac{-i\omega_0}{\nu k_0^2})^{\frac{1}{2}}. \tag{2.74}$$

By retaining only the first order terms in α, a solution for k' can be found. The imaginary part of this solution, which is the spatial damping coefficient α, is given by

$$\alpha = \frac{2k_0}{3\omega_0} \frac{\frac{\omega_0}{2\sqrt{2}} (\frac{\epsilon}{\sigma})^2 (\frac{\omega_0}{\nu k_0})^{\frac{1}{2}} - \frac{\epsilon}{\sigma} (2\nu k_0 \omega_0)^{\frac{1}{2}} + 2\nu k_0^2}{1 - \sqrt{2}\frac{\epsilon}{\sigma} (\frac{\omega_0}{\nu k_0^2})^{\frac{1}{2}} + (\frac{\epsilon}{\sigma})^2 \frac{\omega_0}{\nu k_0^2}}, \tag{2.75}$$

and the real part k'' can be written as

$$k'' = \frac{k_0}{3} \frac{\epsilon}{\sigma} \frac{1 - \frac{\epsilon}{\sigma} (\frac{\omega_0}{2\nu k_0^2})^{\frac{1}{2}} - \frac{2}{\omega_0} (2\nu k_0 \omega_0)^{\frac{1}{2}}}{1 - \sqrt{2}\frac{\epsilon}{\sigma} (\frac{\omega_0}{\nu k_0^2})^{\frac{1}{2}} + (\frac{\epsilon}{\sigma})^2 \frac{\omega_0}{\nu k_0^2}}. \tag{2.76}$$

In the limit of zero elasticity, $\epsilon \to 0$, the damping coefficient reduces to

$$\alpha_0 = \frac{4\eta\omega_0}{3\sigma}, \tag{2.77}$$

which is the damping coefficient for a liquid with a pure surface. For the case of a totally inelastic surface, $\epsilon \to \infty$, α reduces to the damping coefficient obtained by Reynolds [14, 9]:

$$\alpha_\infty = \frac{2k_0}{3\omega_0} \frac{(\nu k_0^2 \omega_0)^{\frac{1}{2}}}{2\sqrt{2}}. \tag{2.78}$$

For determining the temporal damping, waves with a real wavevector k_0 and an imaginary angular frequency ω are considered. The in the low-viscosity limit, ω can be written as

$$\omega = \omega_0 + \omega', \tag{2.79}$$

where $\omega' = \omega'' - i\beta$ represents the change in frequency from the frequency ω_0 of a surface wave of wavevector k_0 in the absence of a monolayer and $\beta \ll \omega_0$ is the temporal damping coefficient. By substituting 2.79 and k_0 in the dispersion relation 2.71, the damping coefficient β can be obtained. By retaining only the first order terms in β and using equation 2.74, the solution for ω' can be acquired. The imaginary part of this solution, which is the temporal damping coefficient β, is given by

$$\beta = \frac{\frac{\omega_0}{2\sqrt{2}} (\frac{\epsilon}{\sigma})^2 (\frac{\omega_0}{\nu k_0})^{\frac{1}{2}} - \frac{\epsilon}{\sigma} (2\nu k_0 \omega_0)^{\frac{1}{2}} + 2\nu k_0^2}{1 - \sqrt{2}\frac{\epsilon}{\sigma} (\frac{\omega_0}{\nu k_0^2})^{\frac{1}{2}} + (\frac{\epsilon}{\sigma})^2 \frac{\omega_0}{\nu k_0^2}}, \tag{2.80}$$

and the real part ω'' can be written as

$$\omega'' = \frac{\omega_0}{2} \frac{\epsilon}{\sigma} \frac{1 - \frac{\epsilon}{\sigma} (\frac{\omega_0}{2\nu k_0^2})^{\frac{1}{2}} - \frac{2}{\omega_0} (2\nu k_0 \omega_0)^{\frac{1}{2}}}{1 - \sqrt{2}\frac{\epsilon}{\sigma} (\frac{\omega_0}{\nu k_0^2})^{\frac{1}{2}} + (\frac{\epsilon}{\sigma})^2 \frac{\omega_0}{\nu k_0^2}}. \tag{2.81}$$

By taking the limit $\epsilon \to 0$, in the case of zero elasticity, the temporal damping coefficient for a liquid with a pure surface is obtained from equation 2.80:

$$\beta_0 = 2\nu k^2. \tag{2.82}$$

The spatial damping coefficient α in equation 2.75 and the temporal damping coefficient β in equation 2.80 are related by

$$\alpha = \frac{\beta}{(\frac{3\omega_0}{2k_0})}. \tag{2.83}$$

Note that equation 2.83 is equal to equation 2.50, which relates the two damping coefficients in the case of a liquid with a pure surface [9].

2.3 Amplitude equation

Just above threshold, the evolution of the system is assumed to be described in terms of the amplitude B of the most unstable mode. The amplitude equation has the form [3]

$$\tau_0 \frac{dB}{dt} = \epsilon_A B - g_0 B^3, \tag{2.84}$$

where $g_0 > 0$ is the self-interaction coefficient, which provides saturation of the wave amplitude. The generic equation 2.84 tells us that the observed damping or growth rate depends on the distance ϵ_A to threshold, where

$$\epsilon_A = \frac{A - A_c}{A_c}. \tag{2.85}$$

In a typical experiment we will create waves at amplitudes A larger than the critical amplitude, and then switch to an amplitude $A < A_c$. The decay is fastest at $A = 0$, however, this is too fast for the camera, whose maximum frame rate is 15 Hz. By switching to a value larger than $\epsilon_A = 0$, the decay will be slower, but then we also have to measure te critical amplitude A_c. This is precisely what is done in the experiment where we will measure both τ_0 and A_c for a pure liquid and a liquid with a monolayer of oil. The temporal damping coefficient β is equal to τ_0^{-1}. From equation 2.84 an expression for the amplitude can be derived,

$$B \sim e^{\frac{\epsilon_A}{\tau_0} t}, \tag{2.86}$$

where

$$\tau^{-1} = \frac{\epsilon}{\tau_0} = \frac{A - A_c}{A_c \tau_0} \tag{2.87}$$

is the decay constant, which is used to determine τ_0.

3 Experimental Setup

3.1 Creating Faraday waves

For the experiments the setup seen in figure 3.1 is used. A Bruël & Kjær vibration exciter is used for the oscillating vertical displacement of the container. The exciter is driven by a NF Electronic Instruments 1930A function generator, which is used to set the frequency and amplitude of the exciter. The frequency used for the experiments is 100 Hz, which corresponds to a wave frequency $\omega = 50$ Hz [3]. The signal of the function generator is amplified by a Bruël & Kjær power amplifier. A circular fluid container with a diameter of 130 mm is used. The fluids used in the experiments are tap water and silicon oil. The silicon oil, Tegiloxan 3, has a low viscosity and surface tension. The relevant properties of Tegiloxan 3 silicon oil and water are listed in tables 3.1 and 3.2 respectively. The silicon oil is used for the monolayer. To create a monolayer a very tiny droplet of oil was dropped on the water surface. The droplet of oil then spreads over the water surface, which creates a layer on the surface. If the drop of oil is tiny enough, it creates a monolayer [2, 7]. Here a pipette is used to put the droplet onto the water surface.

3.2 Measuring wave damping

To measure the wave damping, the following method is used. The amplitude of the function generator is set to a value $A_1 > A_0$, where A_0 is the critical amplitude at which faraday waves are created (see section 2.3). At $t = 0$ the amplitude of the function generator is set to a value $A_2 < A_0$, with the distance to threshold, ϵ_A, close to zero. This slows down the damping of the waves, which is necessary for measuring with the 15 fps camera used. If at $t = 0$ the amplitude is set to zero, a very high speed camera is needed to capture te temporal decay.

Table 3.1: Physical properties of Tegiloxan 3 silicon oil at 21 °C [19].

Density	ρ = 892.4 kg m^{-3}
Viscosity	ν = 3.397 $\cdot$ 10^{-6} m^2 s^{-1}
Surface tension	σ = 18.3 $\cdot$ 10^{-3} J m^{-2}

Table 3.2: Physical properties of water at 20 °C [12].

Density	ρ = 998.2 kg m^{-3}
Viscosity	ν = 1.004 $\cdot$ 10^{-6} m^2 s^{-1}
Surface tension	σ = 72.75 $\cdot$ 10^{-3} J m^{-2}

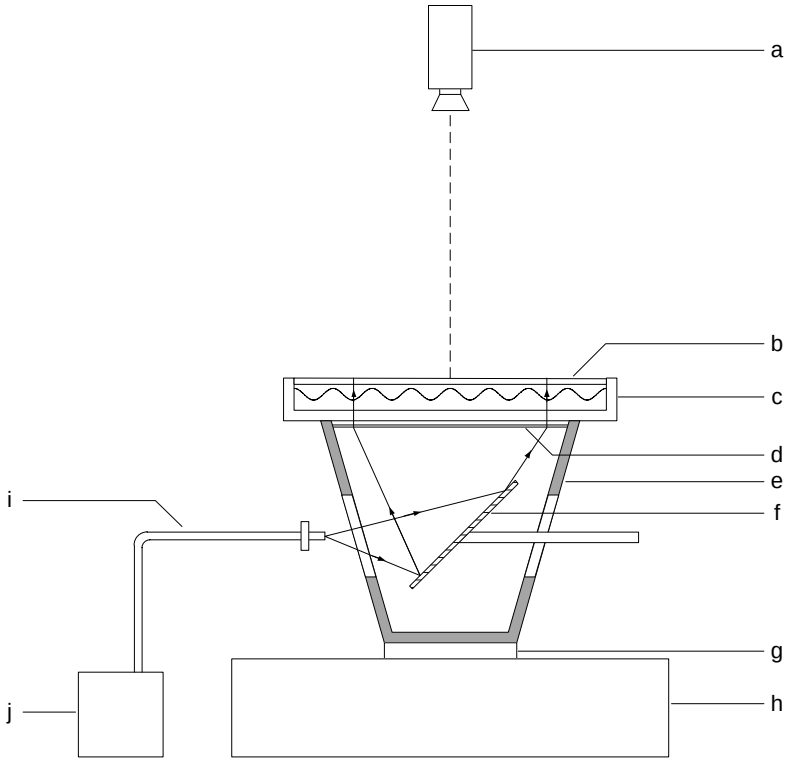

Figure 3.1: The experimental setup. a) CCD Camera, b) frosted glass screen, c) fluid container, d) Fresnel lens, e) cone for supporting the fluid container, f) mirror, g) heat exchanger, h) exciter, i) optical fiber, j) light source.

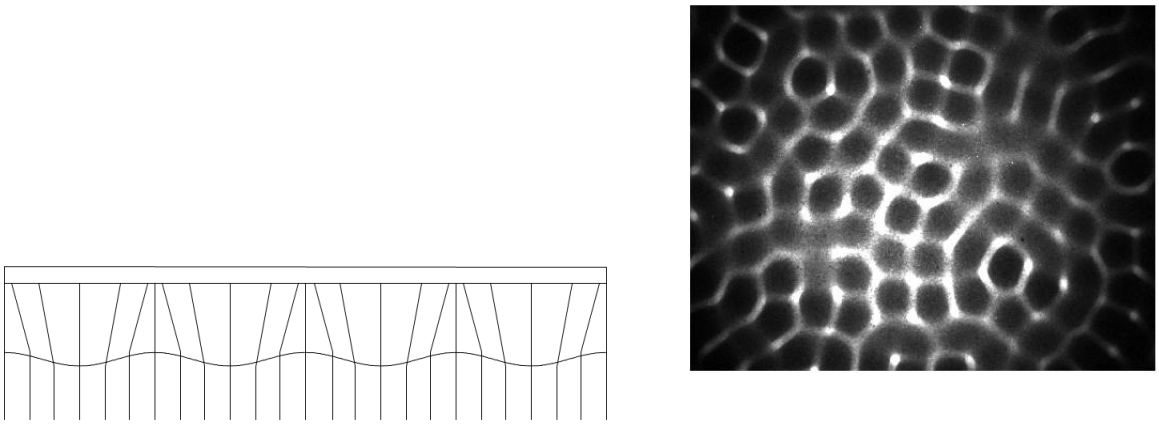

Figure 3.2: On the left side the principal of the shadowgraph technique. On the right side a recorded image using the shadowgraph technique.

3.2.1 Shadowgraphy

To measure the wave damping the shadowgraph technique is used. This technique visualizes the free surface using the refraction of parallel light incident from below. A Fresnel lens is used to create a parallel beam of light. The waves refract the beam of light, which then forms a pattern of bright and dark spots on a screen of frosted glass [19] (see figure 3.2).

An Olympus Highlight 3000 cold light source, an incandescent halogen lamp, illuminates the fluid through an optical fiber. No significant temperature change is observed using this method, so the absorption of light in the fluid may be neglected [19]. The light source is connected to a DC power source to avoid the 100 Hz modulation of the mains AC. An Allied Vision Technologies Dolphin F-145B camera is used to record a series of grayscale images. The camera is synchronized with the function generator and triggered using a custom built frequency divider. The shutter time of the camera is well below the period of the waves, so that the image can be considered as an instantaneous snapshot of the surface. The intensity of the image is the data which will be used in our analysis. Grayscale images consist of pixels with values from 0 to 255, where 0 is black and 255 is white. For a good result saturation should be prevented. Saturation is the loss of intensity information when the signal exceeds to scale described before (see figure 3.3). So, the intensity should be between 0 and 255. This is done be choosing a small diaphragm of the lens and a low shutter time of the camera.

3.2.2 Image processing

From images such as shown in figure 3.2 we want to compute the time-dependent wave amplitude. Clearly the waves are irregular, the image contains noise and the illumination is not uniform. The root-mean square of the image is equivalent to the wave energy spectrum, integrated over all wavenumbers,

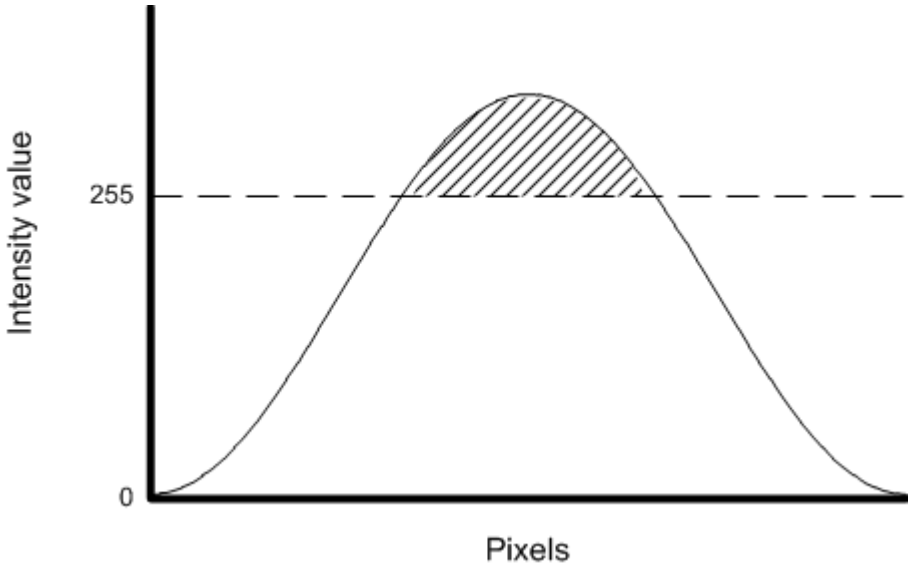

Figure 3.3: An example of saturation. The data above the intensity value 255, above the dashed line, will be lost.

$$I_{rms}(t) =< (I(x, y; t) - < I(t) >)^2 >= \iint dk_x dk_y E(k_x, k_y; t), \tag{3.1}$$

where $<>$ denotes a spatial average. Clearly, I_{rms} is influenced by noise, which we filter by convolving the image with the binomial matrix

$$\mathbf{B}^2 = \frac{1}{16}\begin{pmatrix} 1 & 2 & 1 \\ 2 & 4 & 2 \\ 1 & 2 & 1 \end{pmatrix}, \tag{3.2}$$

which acts as a low-pass filter [18]. After convoluting the image matrix 50 times with equation 3.2 the noise will be eliminated (see figure 3.4).

Finally, we correct each image $I(x, y)$ for the non-uniform illumination by subtracting the background $I_{bg}(x, y)$ with no waves and then divide by it,

$$\tilde{I}(x, y; t) = \frac{I(x, y; t) - I_{bg}(x, y)}{I_{bg}(x, y)}. \tag{3.3}$$

For the image processing MATLAB™ is used, see appendix A for the MATLAB™ script.

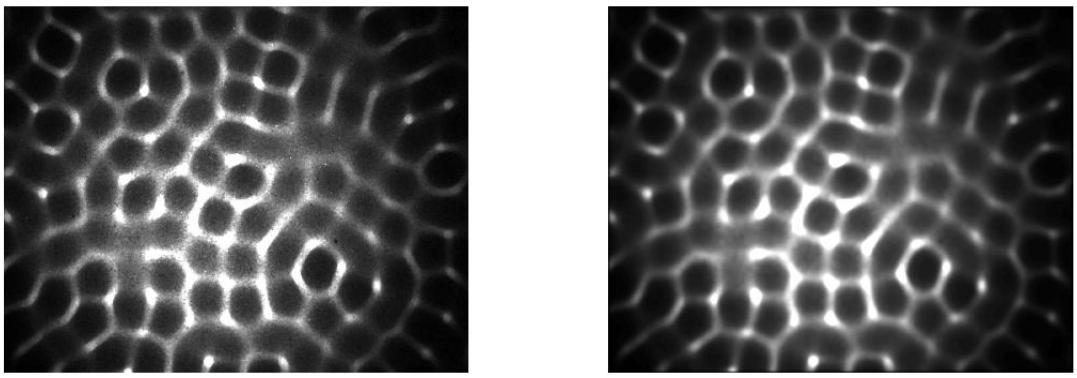

Figure 3.4: The image on the left is the original image. On the right side is the image after convolving 50 times with equation 3.2.

4 Results

In this chapter the results are discussed. First the decay constant for the surface waves is determined and from there the critical amplitude A_c is calculated. Then τ_0 and the temporal damping coefficient are determined. This is done for both water with a clean surface and water covered with a monomolecular film of oil.

4.1 The decay constant

In this section is discussed how to determine the decay constant, τ, from section 2.3. Therefore a result of the damping of water is used as an example, see figure 4.1. The wave amplitudes computed from the corrected images are plotted as function of time until the one but last images. The amplitude I_{rms} does not decay to zero because of noise at both small and large wavenumbers.

Figure 4.2 shows the same graph as in figure 4.1, but with a logarithmic I_{rms} axis. It is seen that the surface wave amplitude decays exponentially. The decay constant can now be calculated by [13]

$$\tau^{-1} = -\frac{d \ln |I_{rms}|}{dt}. \tag{4.1}$$

So, the graphs in figures 4.1 and 4.2 can be plotted with an exponential with the form

$$I_{rms} = I_d + I_0 e^{\frac{t}{\tau}}, \tag{4.2}$$

where I_d allows for the rms difference between images from the same background, I_0 is a measure for the maximum wave amplitude and τ is the decay constant.

4.2 The critical amplitude

To determine te critical amplitude the decay constant at different values of the amplitude of the function generator, $A < A_c$, is calculated. Figure 4.3 shows the damping of the surface waves for water with a pure surface. It can be seen that the damping time increases for an increased amplitude. This is as expected, as an increasing amplitude of the function generator comes closer to the critical amplitude A_c. At A_c, where $\epsilon_A = 0$, it takes infinitely long to create, or damp, the surface waves. For each amplitude five measurements were performed, and the decay constants of these different measurement were averaged. Figure 4.4 shows the decay constant as function of the amplitude of the function generator. By

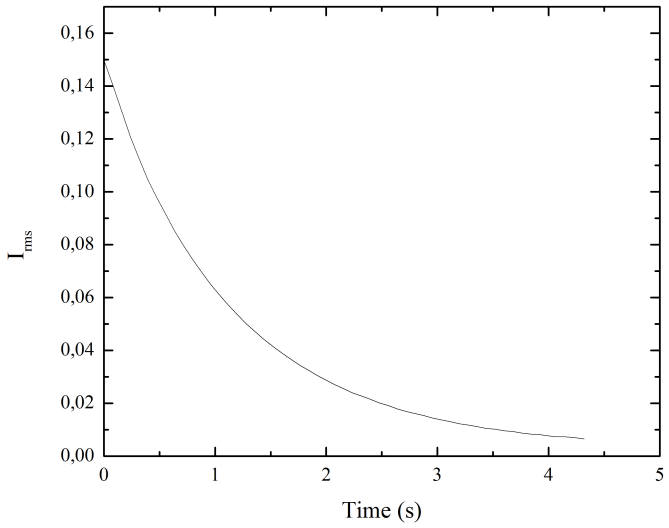

Figure 4.1: The damping of water with a pure surface.

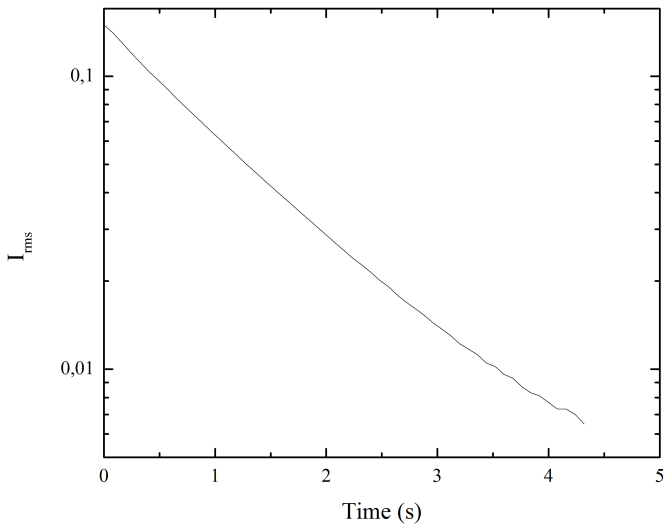

Figure 4.2: The damping of water with a pure surface with a logarithmic I_{rms} axis.

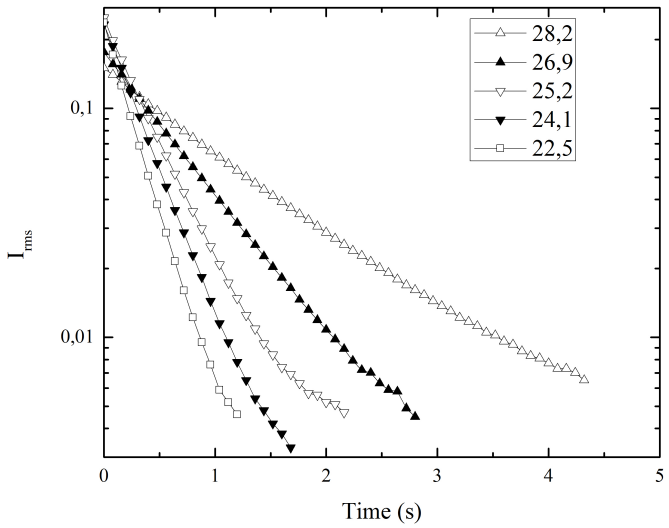

Figure 4.3: The damping of water with a pure surface, for different values of the amplitude of the function generator, with a logarithmic I_{rms} axis.

linearly fitting the data in figure 4.4 the critical amplitude A_c is found. For water with a pure interface this critical amplitude of the function generator is $A_c = 29.9 \pm 0.1$ V. In fact, we are interested in the vertical acceleration of the fluid at the threshold. As the acceleration is not measured in the experiment, we use a reference value for the acceleration at the critical amplitude for a single layer of water. Therefore, the threshold is computed using a linear stability analysis [3, 19, 20]. The computed acceleration at the threshold is 2.56 ms^{-2}. Now the decay constant can be plotted as a function of the acceleration of the exciter, which is seen in figure 4.5. The values of the acceleration are calculated using the reference value computed above.

Figure 4.6 shows the damping of surface waves for water with a monomolecular film of oil. As for the pure case, the damping time increases for an increased value of the acceleration of the exciter. The decay constant is determined as before, and figure 4.7 shows τ^{-1} as function of the acceleration. By fitting the data in figure 4.7 an acceleration at the critical amplitude of water with a monomolecular oil film of 1.34 ± 0.02 ms^{-2} is found. This value is lower than the acceleration at threshold for water with a pure surface. The error in the data of figure 4.7 is fairly large due to the variability from run to run.

4.3 The temporal damping coefficient

In this section the temporal damping coefficients for water with a pure surface and water with a monomolecular layer of oil will be determined from figures 4.5 and 4.7. The decay constant τ^{-1} can be fitted as

$$\tau^{-1} = \frac{A - A_c}{A_c \tau_0} = \frac{A}{A_c \tau_0} - \tau_0^{-1}, \tag{4.3}$$

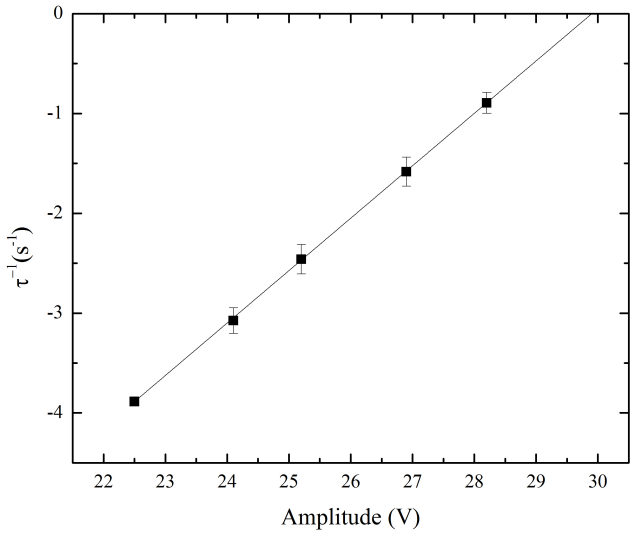

Figure 4.4: The decay constant as function of the amplitude of the function generator for water with a pure surface.

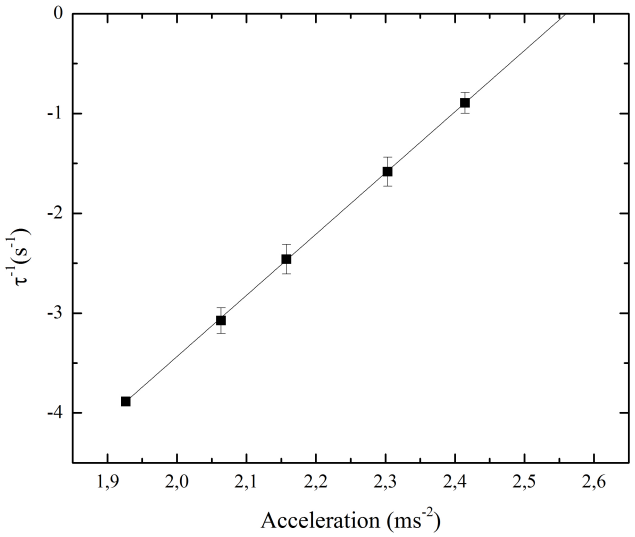

Figure 4.5: The decay constant as function of the acceleration for water with a pure surface.

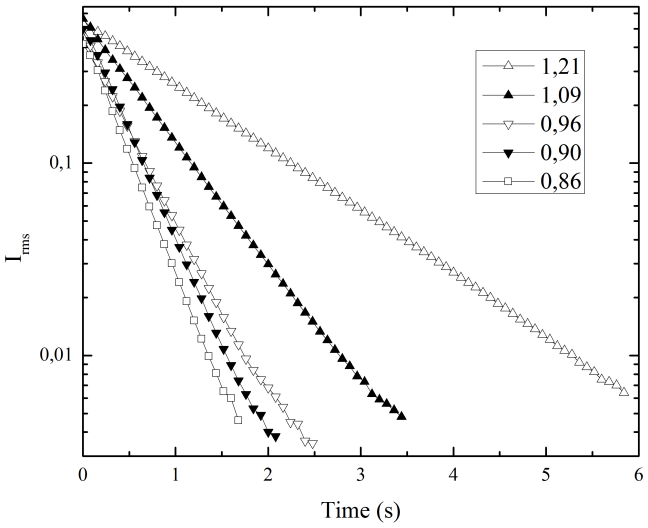

Figure 4.6: The damping of water with a monomolecular film of oil, for different values of the acceleration. The I_{rms} axis is logarithmic.

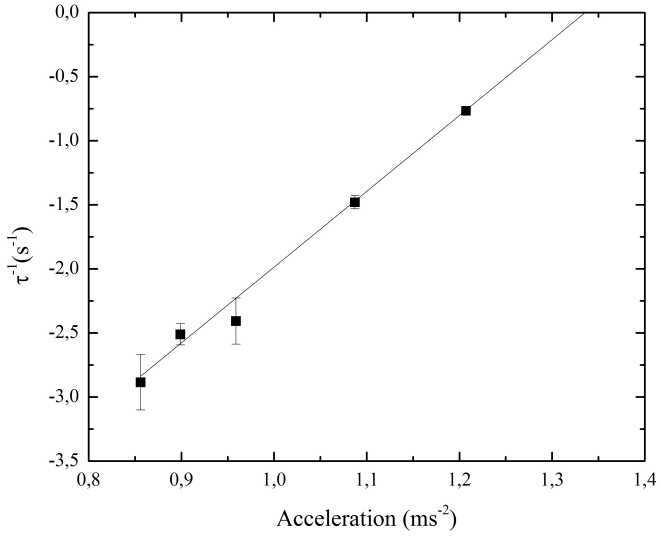

Figure 4.7: The decay constant as function of the acceleration for water with a monomolecular layer of oil.

as found in section 2.3. So, the slopes in figures 4.5 and 4.7 are equal to $\frac{1}{A_c \tau_0}$ and the intercepts with the τ^{-1} axis are equal to $-\tau_0^{-1}$. For water with a pure surface $\tau_0 = (6.4 \pm 0.1) \cdot 10^{-2}$ s and for water with a monomolecular oil film $\tau_0 = 0.13 \pm 0.01$ s. The temporal damping coefficient β is equal to τ_0^{-1}, so for water with a pure surface $\beta = 15.7 \pm 0.2$ s^{-1} is found. For the mono-layered water a value of $\beta = 7.9 \pm 0.2$ s^{-1} is found, which is lower than the value of β of water with a pure surface.

From equation 2.48 the theoretical temporal damping of the pure water case can be calculated. The viscosity ν is obtained from table 3.2 and the wavevector k is measured from the images using a MATLAB™ script that calculates the wavenumbers corresponding to the fundamental frequency for a series of captured images [20]. For the pure water case $k = 1065$ m^{-1} is found. So, the theoretical temporal damping coefficient of the pure water case is $\beta = 2.35$ s^{-1}. This value is lower than the damping coefficient found in the experiment. This could be caused by the damping effect of the sidewalls of the fluid container. By scaling up the experiment, using a larger fluid container and a thicker fluid layer, the damping effect of the sidewalls could be decreased. For calculating the temporal damping coefficient of the monolayered water, equation 2.80, we need to know the surface dilational modulus ϵ. The wavevector, $k = 1082$ m^{-1}, is calculated from the images as before, $\omega_0 = \frac{50}{2\pi}$ rad s^{-1} (see chapter 3) and ν and σ are obtained from table 3.2. Figure 4.8 shows the temporal damping coefficient of water with a monomolecular film as function of ϵ. At $\epsilon = 0$ the damping coefficient is equal to that of the pure case. For all other values of ϵ, β is higher for the monolayered water. In the experiment the damping coefficient of the monolayer case was found to be lower than for the pure case. This is not what we expected, as figure 4.8 shows that it should be higher. This could be caused by an error in the amplitude of the exciter. The results show that the critical amplitude of water with a monomolecular oil film was found to be lower than that for pure water, however we expect it to be a higher value. We should expect that the damping for the monolayer case is higher compared to pure water, so the critical amplitude should be higher as well.

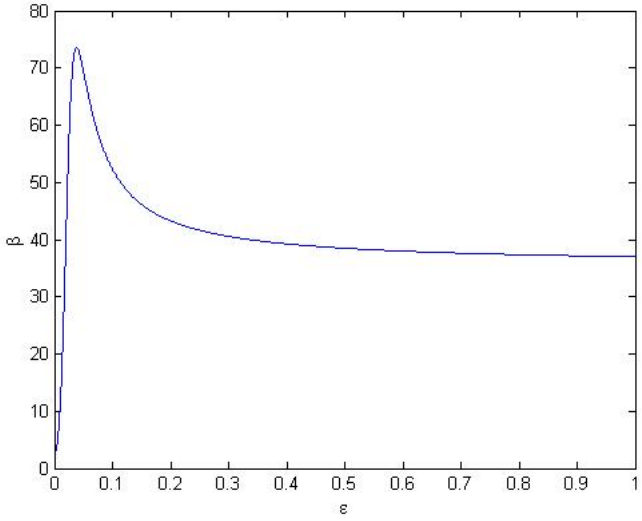

Figure 4.8: The temporal damping coefficient of water with a monomolecular layer of oil as function of the dilational modulus.

5 Conclusion

The goal of this work was the find out the effect of the damping of Faraday waves due to an monomolecular film of oil. The damping of waves due to an oil film is already known for ages, but is still isn't clear what exactly happens. In this report a theory is provided, which gives the effect on the temporal damping coefficient after adding a monomolecular layer of oil on water. Shadowgraphy is used to measure the damping. The images taken in this technique were processed in MATLAB^{TM}, where the unwanted high and low frequency responses were cut out. For both the damping of the pure case as for the mono-layer case, it was found that the damping time increases for values closer to the critical amplitude where $\epsilon = 0$. It was also found that the damping is an exponential function as expected. The critical amplitude of water with a pure surface was found to be higher compared to the critical amplitude of the mono-layer case, however we should expect the opposite due to a higher expected damping of the water with a monomolecular oil film. The temporal damping coefficients calculated from the data for water with a pure surface and water covered with a monomolecular oil film are $\beta = 15.7 \pm 0.7$ s^{-1} and $\beta = 7.8 \pm 0.2$ s^{-1} respectively. The damping coefficient found for the pure water case is higher compared to the theoretical value, which could be caused by the sidewall damping of the liquid container. These damping effects could be decreased by scaling up the experiment. The temporal damping of the monolayered water is expected to be higher than the damping of pure water, however we measured the opposite. A possible cause is an error in the amplitude of the exciter.

Bibliography

[1] Aiken. *Proc. Roy. Soc. Edin.*, 12, 1883.

[2] M.R. Buhaenko, J.W. Goodwin, and R.M. Richardson. Surface rheology of spread monolayers. *Thin Solid Films*, 159:171–189, 1988.

[3] P. Chen and J. Viñals. Amplitude equations and pattern selection in faraday waves. *Phys. Rev. E 60*, pages 559–570, 1999.

[4] J.T. Davies and R.W. Vose. *Proc. Roy. Soc.*, A286, 1965.

[5] B Franklin. Of the stilling of waves by means of oil. *Philosophical Transactions*, vol.64:445–460, 1774.

[6] C.H. Giles. Franklin's teaspoonful of oil. *Chem. Ind.*, 1:1616–1624, 1969.

[7] J. Krägel, G. Kretzschmar, J.B. Li, G. Loglio, R. Miller, and H. Möhwald. Surface rheology of monolayers. *Thin Solid Films*, 284-285:361–364, 1996.

[8] L.D. Landau and E.M. Liftshitz. *Fluid Mechanics*. Pergamon Press, 1959.

[9] K.Y. Lee. *Optical studies of capillary waves at liquid vapor interfaces*. PhD thesis, Harvard University, 1992.

[10] V.G. Levich. *Act. Phys. U.R.S.S.*, 14, 1941.

[11] V.G. Levich. *Physicochemical Hydrodynamics*. Prentice-Hall, 1962.

[12] D. Lide. *CRC Handbook of chemistry and physics*. Taylor and Francis Group, 89th edition edition, 2008.

[13] E.H. Lucassen-Reynder and J. Lucassen. Properties of capillary waves. *Advan Colloid Interface Sci*, 2:347–395, 1969.

[14] J Lyklema. *Fundamentals of interface and colloid science: Liquid-fluid interfaces*. Academic Press, 2000.

[15] S.P. McKenna. *The Influence of Surface Films on Interfacial Flow Dynamics*. PhD thesis, Massachusetts Institute of Technology, 1997.

[16] J. Miles. On faraday waves. *J. Fluid Mech.*, 248:671–683, 1993.

[17] L. Rayleigh. *Proc. Roy. Soc. London*, 47, 1890.

[18] W. Van de Water. Computers bij fysische experimenten, 2009.

[19] M.T. Westra. *Patterns and weak turbulence in surface waves*. PhD thesis, Technische Universiteit Eindhoven, 2001.

[20] T.F.A. Wilms. Parametrically excited surface waves in a two-liquid system, 2009.

A MATLAB™ Script

In this appendix the MATLAB™ script used for processing the images is shown.

```
% filterandintensity_final.m

% Copyright 2011 Johan Merks

% Routine for filtering the images with a binomial filter
% and calculating the intensity.

clear search_string dirs dirs_count IMG data_dir fps t0 tend i j u v;
search_dirs = '*BG*';
search_string = '*.bmp';
data_dir = 'Filtering and Intensity Data BG\'; % Where to store data

fps = 12.5; % Frames per second of the CCD camera
filter = (1/16)*[1 2 1;2 4 2;1 2 1]; % Binomial filter B^2
n_bin = 50; % The number of times the image is filtered

mkdir(data_dir);
dirs = dir(search_dirs);
dirs_count = size(dirs);

t0 = cputime;

for j=1:1:dirs_count(1)
    clear dirlist length IMG IMG2 int_E BG_IMG dim_BG_IMG int_E_dl_bg time;
    dirlist = dir([dirs(j).name '\' search_string]);
    length = size(dirlist);

    display('Number of files:');
    display(length);

    % The background image, the last image in the measurement
    BG_IMG = double(imread([dirs(j).name '\' dirlist(length(1)).name]));

    % Filtering and resizing routine for the background image
    for v=1:1:n_bin

        % Convulating the matrices 'filter' and 'BG_IMG'
        BG_IMG = conv2(filter,BG_IMG);
```

```
        % Resizing the image matrix to its original dimensions
        BG_IMG(:,1)=[];
        BG_IMG(1,:)=[];
        dim_BG_IMG=size(BG_IMG); % Dimensions of the BG_IMG matrix
        BG_IMG(:,dim_BG_IMG(2))=[];
        BG_IMG(dim_BG_IMG(1),:)=[];
    end

    for i=1:1:length(1)-1
    % The last image is used as the background image,
    % so it is not taken into the rest of the routine
        clear IMG IMG2 IMG_dif av_IMG_dif dim_IMG2;
        IMG = double(imread([dirs(j).name '\' dirlist(i).name]));
        IMG2=IMG;

        % Image filtering and resizing routine
        for u=1:1:n_bin

            % Convulating the matrices 'filter' and 'IMG2'
            IMG2 = conv2(filter,IMG2);

            % Resizing the image matrix to its original dimensions
            IMG2(:,1)=[];
            IMG2(1,:)=[];
            dim_IMG2=size(IMG2); % Dimensions of the IMG2 matrix
            IMG2(:,dim_IMG2(2))=[];
            IMG2(dim_IMG2(1),:)=[];
        end

        % Difference of IMG2 and the background image.
        IMG_dif = IMG2 - BG_IMG;
        % The average value of the intensity.
        av_IMG_dif = mean(mean(IMG_dif));

        % Integral E(kx,ky) dkx dky
        int_E(i) = sqrt(mean(mean((IMG_dif-av_IMG_dif).^2)));

        time(i)=i/fps;

    end
        % int_E divided by the mean BG_IMG,
        % making int_E_dl_bg dimensionless.
        int_E_dl_bg = int_E/mean(mean(BG_IMG));

        % Store the calculated parameters for all the files
        % in directory xxV in the file xxV.mat.
        save([data_dir dirs(j).name '.mat'],'int_E','int_E_dl_bg','time');
end

tend = cputime - t0; % Total time needed to complete the routine.
```